Catalysis Science & Technology

PAPER

View Article Online
View Journal | View Issue



Cite this: *Catal. Sci. Technol.*, 2017, 7, 894

# Unusual deactivation of HZSM-5 zeolite in the methanol to hydrocarbon reaction†

Liang Qi,[ab] Jinzhe Li,[a] Linying Wang,[a] Lei Xu*[a] and Zhongmin Liu*[a]

Received 24th November 2016,
Accepted 4th January 2017

DOI: 10.1039/c6cy02459a

rsc.li/catalysis

Temperature-programmed methanol to hydrocarbon (TP-MTH) reactions were performed over HZSM-5 zeolite to monitor the change of reaction performance along with reaction temperature in order to understand the mechanistic reason for the temperature influence on the reaction. With a gradual increase of reaction temperature (0.5 °C $min^{-1}$), the MTH reaction could evolve from the induction period with low methanol conversion to the state with 100% methanol conversion. Four different reaction stages could be clearly observed: the initial reaction stage, the auto-catalysis reaction stage, the deactivation stage and the activity recovery stage. An unusual deactivation behavior was observed following the auto-catalysis period. Further investigations revealed that 1,2,3,5-tetraMB was the main active species during the initial autocatalytic stage and its "overloading" effect resulted in the unusual deactivation phenomenon, *i.e.* despite its high intrinsic reactivity, too quick formation of poorly mobile 1,2,3,5-tetraMB and lower methylbenzenes will lead to the occupation of most catalyst channels and channel intersections and cause the deactivation of HZSM-5 at low temperature. Further study demonstrated that the "overloading" effect could be alleviated or eliminated by enhancing the catalyst diffusivity or decreasing the acid site density of the zeolite catalyst.

## 1. Introduction

Methanol-to-hydrocarbon (MTH) conversion over acid zeolites has attracted great interest for the production of gasoline or basic chemicals from nontraditional carbon-based resources.[1–4] Commercialization of related processes such as methanol-to-gasoline (MTG), methanol-to-olefins (MTO), and methanol-to-propene (MTP) has made remarkable progress in recent years, however, the mechanisms related to product formation and/or catalyst deactivation are still not well understood due to the complexity of the reaction system.

The MTH reaction proceeds *via* a "hydrocarbon pool" (HCP) mechanism,[2,5–7] in which the composite of zeolite and HCP compounds within the channels and/or cages is considered to be the catalysis center.[2,5–9] Accordingly, carbenium ions formed by the protonation of retained organics are the most important reaction intermediates.[10–22] Over ZSM-5 zeolite, further research demonstrated that both polymethylbenzenes and olefins can act as active HCP species and a "dual-cycle" mechanism was proposed,[6,7] suggesting that the propene/ethene selectivity can be tuned by adjusting the contribution of the two cycles.[6,7,23]

The generation and evolution of HCP species have an ultimate influence on the catalyst activity. MTH conversion is an autocatalytic reaction and can be divided into an induction period, high conversion period and deactivation period considering the change of methanol conversion with reaction time.[2,4,24] The induction period should be closely related to the formation of the first C–C bond and the initial HCP compound.[25–27] After the formation of the initial active species, more HCP species will subsequently be formed in an autocatalytic way and the zeolite can be transformed into a highly active catalyst when a sufficient amount of active species is generated. At high temperature, a dynamic equilibrium on the reaction center can be reached between the carbon chain growth and the product elimination, which brings about the pseudo steady-state period.[24,28,29] Meanwhile, during the high conversion stage, besides the active retained species, some inactive and poorly mobile retained species and coke species will be unavoidably generated and gradually cause the blockage of zeolite channels, leading to the final catalyst deactivation.[12,30] The active HCP species could promote the activity while the inactive retained species or coke

[a] *National Engineering Laboratory for Methanol to Olefins, Dalian National Laboratory for Clean Energy, iChEM (Collaborative Innovation Center of Chemistry for Energy Materials), Dalian Institute of Chemical Physics, Chinese Academy of Sciences, Dalian 116023, People's Republic of China. E-mail: leixu@dicp.ac.cn, liuzm@dicp.ac.cn; Fax: +86 411 84379998; Tel: +86 411 84379998*

[b] *University of Chinese Academy of Sciences, Beijing 100049, People's Republic of China*

† Electronic supplementary information (ESI) available. See DOI: 10.1039/c6cy02459a

species should be responsible for the deactivation for the MTH catalyst.[2,12]

MTH conversion is a considerably temperature-dependent reaction.[31–37] The catalyst activity and product selectivity change obviously with reaction temperature even on the same zeolite catalyst;[31–33,35,37] the generation rate of the initial HCP species is very sensitive to reaction temperature and thus the induction period can be varied evidently by slightly changing the reaction temperature; and the deactivation as well as the lifetime of the catalyst changes greatly with reaction temperature.[7,35,36,38,39] Our previous work has illustrated that, over zeolites having small cages like SAPO-35, SAPO-34 and SAPO-18, the catalyst could also be deactivated at low reaction temperatures due to the formation of adamantane hydrocarbons, whereas at high temperatures the deactivation was caused by the accumulation of polycyclic aromatics.[34,36] The retained species of the MTH reaction changed with reaction temperature over H-SSZ-13 zeolite: at low reaction temperatures (573–598 K) the main active species were methylated benzene carbocations, which changed to methylated naphthalene carbocations at high temperatures (623–723 K).[37] These findings imply that the reaction temperature change should cause some changes in reaction paths and reaction mechanisms. Given the importance of temperature in the MTH reaction, it is interesting to monitor the change of reaction performance and the catalyst along with reaction temperature in order to understand the whole reaction network and the mechanistic reason for the temperature influence on the reaction.

In the present work, temperature-programmed MTH (TP-MTH) reactions were performed over HZSM-5 zeolite. With a gradual increase of reaction temperature (0.5 °C $min^{-1}$), the MTH reaction could evolve from the induction period with low methanol conversion to the state with 100% methanol conversion. Interesting new phenomena were observed and detailed investigations were further carried out, which leads to the proposal of the unusual deactivation by the "overloading" effect of the active species during MTH conversion over the HZSM-5 zeolite.

# 2. Experimental section

### 2.1 Preparation of the catalysts

HZSM-5 samples (Si/Al = 19, 21 and 99) (designated as HZ-19, MZ-21 and HZ-99) were obtained from the Catalyst Plant of Nankai University.

Another nano-crystalline zeolite with a Si/Al ratio of 20 was synthesized in our laboratory according to previous reports.[40] The calcined sample was ion exchanged with a 1 M (1 mol $L^{-1}$) $NH_4NO_3$ aqueous solution for 2 h at 80 °C followed by washing with deionized water for 1 h at 70 °C twice. Then the samples were dried at 120 °C for 12 h and calcined in air at 550 °C for 10 h. The final protonated sample was denoted as NZ-20.

### 2.2 Characterization of the catalysts

The powder XRD pattern was recorded by a PANalytical X'Pert PRO X-ray diffractometer with Cu-Kα radiation ($\lambda$ = 1.54059 Å), operating at 40 kV and 40 mA. The chemical composition of the samples was determined with a Philips Magix-601 X-ray fluorescence (XRF) spectrometer. The crystal morphology and structure were observed by field emission scanning electron microscopy (Hitachi, SU8020).

$N_2$ adsorption–desorption isotherms were obtained using a Micrometrics ASAP 2020 system at 77 K.

The acid properties were examined by means of temperature-programmed desorption of ammonia ($NH_3$-TPD). The experiment was carried out with Autochem 2920 equipment (Micromeritics). The calcined samples were pretreated at 550 °C for 1 h in a helium atmosphere and then saturated with ammonia at 100 °C for 30 min. After purging with helium, the samples were heated at 10 °C $min^{-1}$ from 100 °C to 700 °C for desorption.

Diffuse reflectance UV/vis spectra (DRUV/vis) were recorded with a Varian Cary 5000 spectrophotometer to characterize the entrapped species on the catalysts.

The total amount of retained species on the catalysts was determined using the TGA method by heating the sample from 150 °C to 700 °C with a heating rate of 5 °C $min^{-1}$ in an atmosphere of 10 mL $min^{-1}$ $O_2$ combined with 10 mL $min^{-1}$ $N_2$. Before measurement, the sample was heated to 200 °C with a heating rate of 10 °C $min^{-1}$ and maintained for 10 min in an atmosphere of 20 mL $min^{-1}$ $N_2$ to remove the physically adsorbed water, and then the temperature was cooled down to 150 °C and maintained for another 10 min.

### 2.3 Catalytic studies

The reactions were performed in a fixed-bed stainless steel tubular reactor (9 mm i.d.) at atmospheric pressure. The catalysts were pressed into tablets, crushed and sieved into a fraction of 40–60 mesh. 1 g of catalyst sample was used in all experiments. To get a plug flow of the mixed feed, quartz sands were added to the upper and lower part of the reactor. The catalyst was activated *in situ* with an air flow (20 mL $min^{-1}$) at 550 °C for 2 h before being adjusted to a predetermined reaction temperature. For the TP-MTH reaction, the reaction temperature was increased at a heating rate of 0.5 °C $min^{-1}$.

Methanol was fed into the reactor at a weight space velocity of 4 $h^{-1}$ with a pump. For the toluene co-feeding experiment, a mixture of methanol and toluene was directly used as the reactant. In order to avoid liquefaction of the product, the outlet line was twined with heat tape to keep the temperature at 240 °C. The effluent was analyzed by an on-line gas chromatograph (Agilent GC7890A) equipped with a FID detector and a PoraPLOT Q-HT capillary column.

### 2.4 Extraction and GC-MS analysis of the confined organics

Organic compounds trapped in the catalyst were obtained by dissolving the catalyst (50 mg) in 1.0 mL of 15% HF in a screw-cap Teflon-lined vial. The organic phase was extracted

by $CH_2Cl_2$, and then analyzed using an Agilent 7890A/5975C GC/MSD.

### 2.5 $^{13}$C MAS NMR measurement of HCP species

The same as the conditions for temperature-programmed $^{12}$C MTH reaction, $^{13}$C-methanol was fed into the reactor until the reaction temperature reached a predetermined value. After the reaction, the catalyst was cooled very quickly by putting it into a vessel containing liquid nitrogen. The catalyst was transferred to an NMR rotor in a glove box without exposure to ambient air for $^{13}$C solid-state NMR measurement.

### 2.6 $^{12}$C/$^{13}$C-methanol switch experiments

In the $^{12}$C/$^{13}$C-methanol switch experiments, after the reaction temperature reached the predetermined temperature with $^{12}$C-methanol during the TP-MTH reaction, the feeding line was switched to $^{13}$C-methanol for further 1.5 min. The isotopic distributions of the effluent products and the materials confined in the catalyst were determined by GC-MS (Agilent 7890/5975C) after extraction.

## 3. Results and discussion

### 3.1 Reaction behavior and unusual deactivation during the TP-MTH reaction

The reaction results over HZ-19 during the TP-MTH reaction are shown in Fig. 1. Almost no conversion was observed at relatively low temperature. This is consistent with an earlier report about the existence of an obvious induction period at low reaction temperature, during which sufficient HCP species should be formed and accumulated to trigger an obvious MTH reaction.[24] An apparent MTH reaction could be observed when the reaction temperature was higher than 277 °C and the corresponding methanol conversion was greater than ~4%. As the reaction temperature rose continuously, the autocatalytic MTH reaction was initiated.

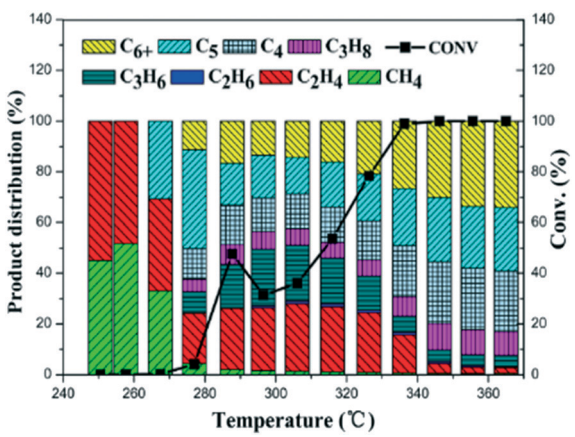


Fig. 1 Methanol conversion and product distribution as a function of temperature during the TP-MTH reaction over the HZ-19 catalyst.

The product distribution variation with reaction temperature during the TP-MTH reaction is shown in Fig. 1. The main products during the induction period were methane and ethene which were similar to our previous result.[24] Propene, $C_4$, $C_5$ and $C_6$+ products could be detected after the initiation of autocatalysis reaction. The selectivity to $C_6$+ species increased firstly and then decreased at around 300 °C and after that, it increased gradually again with the increase of reaction temperature.

Due to the shape-selective effect of ZSM-5 channels, the product distribution of the MTH reaction not only depends on the reaction mechanism but also on the product diffusivity. It is generally recognized that a large molecule diffuses slowly and the diffusivity difference between different molecules may become smaller at higher temperature. The lower selectivity to $C_4$, $C_5$, and $C_6$+ products at a lower temperature range indicates that their selectivity might be controlled by diffusion limitation.

During the whole TP-MTH reaction from low to high temperatures, four different reaction stages could be clearly observed: the initial reaction stage, the auto-catalysis reaction stage, the deactivation stage and the activity recovery stage. This integrated reaction phenomenon is not easily observed under sole low-temperature or high-temperature isothermal conditions.

After the autocatalysis stage, there existed a deactivation stage followed by an activity recovery stage during the TP-MTH reaction. The methanol conversion firstly increased to about 50% at 277 °C and then decreased to 30% at 287 °C. The catalyst activity recovered with a further increase of temperature and complete methanol conversion was obtained at 337 °C. It is not easy to understand why there was an unexpected activity decrease after the autocatalysis reaction already initiated. The TP-MTH reaction results also imply that there should be some change in the ZSM-5 zeolite catalyst. In the case of the SAPO-34 catalyst, we observed that the catalyst could be deactivated at lower temperature by methyladamantane occupying most cages of SAPO-34.[34,36] However, in the present case of ZSM-5 zeolite, a well-known stable catalyst without cages in its framework structure, a similar reason may not be possible since we could not find any methyladamantane on the deactivated catalyst. Further detailed monitoring and characterization of the catalyst during the reaction is necessary to understand the unusual reaction behavior.

### 3.2 Evolution of HCP species and their role at different reaction stages

The organic species retained in the catalyst at different reaction stages were analyzed by GC-MS (after extraction) and UV-vis spectroscopy. The results are shown in Fig. 2, where typical reaction stages were represented by the temperature of 277, 287, 297, 307, 317 and 327 °C, respectively (the samples were denoted as HZ19-277, HZ19-287, HZ19-297, HZ19-307, HZ19-317 and HZ19-327, correspondingly).

 

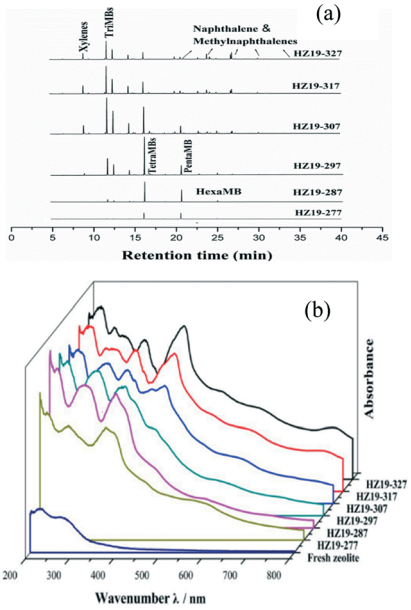


**Fig. 2** GC-MS (a) and UV/vis (b) analysis of retained species at different temperatures during TP-MTH reaction.

As shown in Fig. 2(a), at 277 °C (HZ19-277) tetramethylbenzenes (tetraMBs) and pentamethylbenzene (pentaMB) appeared as the first retained organics. Their amounts, especially for tetraMBs (mainly 1,2,3,5-tetramethylbenzene), increased gradually with the increase of temperature and reached a maximum at 297 °C. Trimethylbenzenes (triMBs) could be detected at 287 °C and their amount increased obviously when the temperature further increased to 297 °C and 307 °C. A small amount of methylnaphthalenes (MNs) was also detected at 297 °C. It seems that the total amount of all retained organics increased to a maximum at ~297 °C, the point where the catalyst started to deactivate.

Fig. 2(b) shows the result of UV/vis spectra characterization. For HZ19-277 and HZ19-287, a rapid increase in the UV/vis bands at 260, and 350 nm was observed due to the accumulation of initial organic HCP compounds. As the reaction progressed to 297, 307, 317 and 327 °C, additional bands occurred at 280, 320 and 420 nm, and the band intensities at ~420 nm increased. On the basis of earlier UV/vis studies of organic compounds on acidic zeolite catalysts,[22,41–45] the bands at 260 and 280 nm were assigned to UV/vis-sensitive dienes and polyalkylaromatics,[45] respectively, and the bands at ~400 nm hint at the formation of polycyclic aromatics.[42,46] The UV-vis results corresponded well with the GC-MS results.

$^{13}$C ssNMR was employed to identify the reaction intermediates and corresponding carbenium ions formed during the TP-MTH reaction under continuous-flow $^{13}$C-methanol conversion (Fig. S1(a)†). The strong $^{13}$C signals between 10 and 50 ppm and that at 127 and 136 ppm indicate the presence of alkylated aromatics such as methylbenzenes.[47] Besides the stable organic species mentioned above, the characteristic signals at 244, 249 and 155 ppm indicating the formation of polymethylcyclopentenyl cations were also observed.[20,48,49] The retained methylcyclopentadiene compounds in the HZSM-5 catalyst were also found in the GC-MS chromatogram (Fig. S1(b)†). These deprotonated forms of methylcyclopentenyl cations confirmed the formation of the polymethylcyclopentenyl cations.

$^{12}$C/$^{13}$C-methanol switch experiments were carried out to distinguish the reactivity of trapped HCP species in the catalyst at 287 °C, and the temperature for the maximum methanol conversion was obtained before deactivation. The total $^{13}$C contents of the retained organics on the catalyst and effluent alkenes after the switch experiments are shown in Table 1. Among the retained organics, tetraMBs, pentaMB, trimethylcyclopentenyls (triMCPs), 1,1-dimethyl-2-ethyl-cyclopentenyls (1,1-diM-2-E-CP), and pentamethylcyclopentenyl (pentaMCP) exhibited higher $^{13}$C content than other retained organics, implying their high activity as important intermediates during the induction period of the reaction on the HZSM-5 zeolite.

The dominant retained species at 287 °C was 1,2,3,5-tetraMB (Fig. 2a), which seems more likely to reside within the ZSM-5 channels due to its bulkier size than other tetraMBs.[7] 1,2,3,5-tetraMB has been successfully identified as one of the major working HCP compounds and proved to participate in the catalytic cycle to produce propene through a paring route.[48–50] As a result, the increase of the initial catalyst reactivity during the initial two stages should be mainly due to the formation and accumulation of highly reactive species related to 1,2,3,5-tetraMB under the current conditions.

### 3.3 Reasons for the deactivation during the TP-MTH reaction

It was recently reported that naphthalene species could lead to catalyst deactivation at low temperature over the HSSZ-13 catalyst.[37] Although the concentration of naphthalene species was quite low in the present case, we still try to understand the relationship between the formation of naphthalene and the unusual deactivation. As naphthalene formation is preferred at high temperature, we monitored the TP-MTH reaction by co-feeding of a small amount of toluene (0.01 wt% and 0.05 wt%) to shorten the induction period and enhance the activity at lower temperature (Fig. S2(a)†). In this case no naphthalene species could be detected in the retained species and 1,2,3,5-tetraMB was still the major constituent (Fig. S2(b)†). However, it can be seen that there also existed deactivation behaviors and the deactivation point also appeared at even lower temperatures. Thus it can be confirmed that the deactivation was not caused by the naphthalene species.

We further analyzed the catalyst after the TP-MTH reaction by TGA in the temperature range of 150–700 °C. Almost all samples showed weight loss at above 200 °C due to the decomposition or combustion of organic species. According to Fig. 3(a) and the DTG result in Fig. S3,† two stages of weight loss could be observed at temperatures higher than 297 °C (HZ19-297). Considering the corresponding GC-MS results, the weight loss at lower temperature was due to the combustion or transformation of methylbenzenes while that at

**Table 1** The total $^{13}C$ content of the retained organics and the effluent products after the $^{12}C/^{13}C$ switch experiment over HZSM-5 at 287 °C with $^{12}C$-methanol feeding during the TP-MTH reaction, followed by 1.5 min of $^{13}C$-methanol feeding

| Retained species | TriMCP | TetraMCP | pentaMCP | Xylenes | TriMBs | TetraMBs | pentaMB | HexaMB |
|---|---|---|---|---|---|---|---|---|
| | 45 | 53.5 | 47.3 | 40.2 | 38.8 | 47 | 58.5 | 21.4 |
| Effluent species | Ethene | | Propene | | Butene | | Pentene | |
| | 48.8 | | 47.3 | | 43.9 | | 39 | |

higher temperature should be caused by the combustion of the later formed methylnaphthalenes.

The total amount of retained species formed at different temperatures is shown in Fig. 3(b). The amount of organic species deposited on HZ-19 samples firstly increased from 277 to 297 °C and then decreased when the temperature was higher than 317 °C. Fig. S4† presents the amount of retained species formed at different reaction temperatures under isothermal conditions. The amount of retained species also differed obviously at different temperatures. At around 300 °C, the amount of retained species was highest, whereas when the temperature was above 320 °C, the amount of the retained species decreased rapidly.

As indicated above, the main retained species was 1,2,3,5-tetraMB. This is different from previous reports on the deactivation of HZSM-5 catalysts at low reaction temperature by the accumulation of bulky and poorly mobile compounds like ethyl-trimethylbenzenes and isopropyl-dimethylbenzenes.[30,35] Considering that all of the organic species should be retained in the catalyst channels, if we take the molecular weight of 1,2,3,5-tetraMB as the average molecular weight of the retained species, it could be calculated that there was about $6.91 \times 10^{-4}$ mol of 1,2,3,5-tetraMB retained in the HZ19-297 sample. For the HZSM-5 (Si/Al = 19) catalyst, the number of channel intersections is $6.96 \times 10^{-4}$ mol $g_{cat}^{-1}$ (about four channel intersections for every unit cell),[51] corresponding to one 1,2,3,5-tetraMB molecule per channel intersection. It seems that the internal space of the catalyst was seriously occupied at 297 °C.

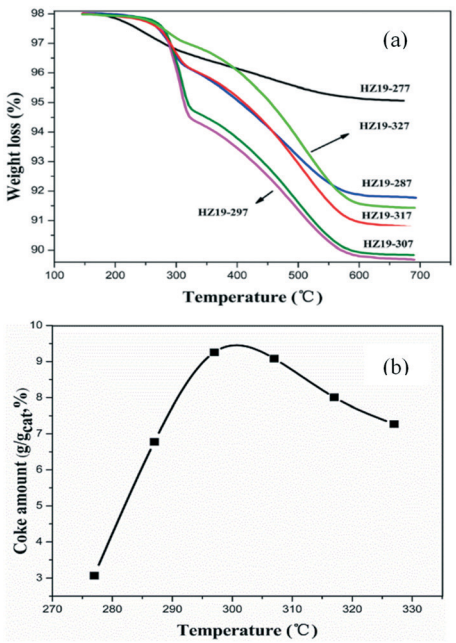


**Fig. 3** TG analysis of retained materials (a) and change of the total coke amount with temperature obtained from TG results (b) during TP-MTH reaction.

Taking all the analysis above into consideration, we propose an assumption that there may exist an "overloading" effect for the HCP species. As illustrated in Scheme 1, during the whole reaction process, after generation and accumulation of the initial HCP species, more HCP species will be generated in an autocatalytic way. When an adequate amount of HCP compounds was accumulated, they can act as reactive centers and accelerate the MTH reaction obviously. However, due to the too rapid generation of aromatic species and the poor diffusivity of primary olefins at relatively low temperature, too many poorly mobile compounds would be generated, retained and occupy most of the catalyst channels or the channel intersections thereafter, which would prevent the reaction of the retained species with methanol and cause the following deactivation behavior in the TP-MTH reaction.

As the TP-MTH reaction proceeded, the activity recovery stage was observed when the temperature was higher than 320 °C. During this stage, the decomposition (or transformation) rate of the retained aromatics and the diffusivity of the effluent products would both be continuously enhanced with increasing temperature which led to the decrease of the amount of the retained species (Fig. 3(b)). This would further help regenerate enough space for the reaction of methanol with the retained species and bring about the recovery of the catalyst activity.

In order to further verify our proposal, we prepared two pre-coked samples based on the same catalyst. Both samples were pre-coked during the TP-MTH reaction but stopped at 277 °C and 297 °C (the deactivation point), respectively. According to the characterization results in Fig. 3(b), the total

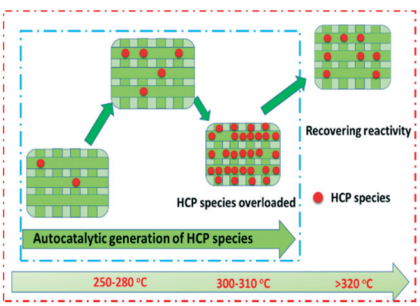


**Scheme 1** Illustration of the HCP species "overloading" effect.

amount of coke species on HZ19-297 was almost three times higher than that on HZ19-277. The TP-MTH reaction was carried out over these two catalysts (temperature rises from 240 °C) and the result is pictured in Fig. 4. For the TP-MTH reaction over the HZ19-277 catalyst, the promoting effect of the pre-formed retained species on the MTH reaction was quite obvious. Compared with the fresh one, HZ19-277 possessed a much higher initial activity and the deactivation point was also advanced. However, for HZ19-297, a weak autocatalytic effect of the pre-formed aromatics can only be observed initially and the increasing rate of methanol conversion was even slower than that over the fresh catalyst. Consequently, the "overloading" effect can be shown clearly over the HZ19-297 catalyst due to the excessive introduction of aromatic species.

When the catalyst was overloaded with the HCP compounds, most parts of the crystals and the molecules therein would become inaccessible to incoming methanol after deactivation. This indicated that these retained species would participate much less in the HCP cycle which can be reflected through the isotopic switch experiment.[52] To monitor the reactivity change of the retained species, additional $^{12}C/^{13}C$ switch experiments were carried out at 297 °C (the deactivation point) and 327 °C (one of the activity recovery points) (the detailed value of the $^{13}C$ content is given in Table 2). At 297 °C tetraMBs lost most of their reactivity, and xylenes and triMBs almost totally changed to inactive species. This presented a clear demonstration of the "overloading" effect of methylbenzene species. Interestingly, during the activity recovery stage (>320 °C), all the tested retained species became active again and the reactivity seemed even higher than that observed in Table 1. Compared with the results of Tables 1 and 2, the $^{13}C$ content of pentaMB became a little lower indicating a small decrease of the reactivity while that of hexaMB remained almost unchanged. Considering the molecular size of pentaMB and hexaMB, the present results suggest that they possibly existed near the external surface of HZSM-5 crystals.

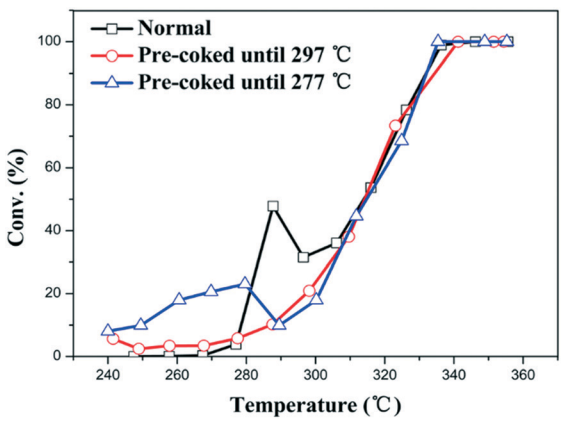


Fig. 4 Methanol conversion as a function of temperature during the TP-MTH reaction for the fresh catalyst and pre-coked catalysts during the TP-MTH reaction until the reaction temperature reached 277 °C and 297 °C.

Table 2 The total $^{13}C$ content of the retained organics and the effluent products after the $^{12}C/^{13}C$ switch experiment over HZSM-5 at 297 °C and 327 °C with $^{12}C$-methanol feeding during the TP-MTH reaction, followed by 1.5 min of $^{13}C$-methanol feeding

| Retained species | Xylenes | TriMBs | TetraMBs | pentaMB | HexaMB |
|---|---|---|---|---|---|
| 297 °C | 0.55 | 1.15 | 12.76 | 48.66 | 29.60 |
| 327 °C | 45.73 | 47.82 | 59.97 | 60.39 | 27.66 |

### 3.4 Alleviation of the "overloading" effect during the TP-MTH reaction

The "overloading" effect was caused by accumulation of too much methylbenzene. The accumulation rate of the retained aromatics should be closely related to the balance of their formation rate and their diffusion rate. In order to alleviate or eliminate the "overloading" effect, we can either decrease the formation rate of the retained species or enhance the diffusion properties of the catalyst. The formation rate is closely related to the acid properties, and the diffusion property is closely related to the crystal size.

We choose another three HZSM-5 catalysts to test the above idea: one HZSM-5 catalyst (Si/Al = 99) with a similar crystal size but different Si/Al ratio (the acid site density is much lower than that of HZ-19 and the characterization information of the samples has been presented in our previous work[39]), and two HZSM-5 zeolites exhibiting micro (MZ-21) and nano (NZ-20) range crystal size but with similar acid properties (Fig. S5 and S6†). The NZ-20 sample presented a pure and well crystallized MFI phase (Fig. S7†) with a crystallite size of 20–50 nm while the MZ-21 sample presented a crystallite size of 2 um (Fig. S5†). For MZ-21 and NZ-20 samples, the Si/Al ratios were almost the same but the external surface area of the NZ-20 catalyst was much higher, indicating its better diffusion characteristics (Table S1†).

The activities of HZ-99, NZ-20 and MZ-21 catalysts were tested under temperature-programmed conditions. The "overloading" effect was eliminated on the HZ-99 catalyst which is due to the much lower formation rate of the retained species (the GC-MS and TG analysis of the corresponding retained species has been presented in the previous work[39]). For the MZ-21 catalyst, the reaction phenomenon was almost the same as that for HZ-19. Because of the higher exposure degree of active sites for the NZ-20 catalyst, the formation of the initial HCP species was much easier and a shorter induction period was observed (Fig. 5). The methanol conversion increased continuously with the increase of temperature. Although the increasing rate of methanol conversion slowed down at around 300 °C, no deactivation behavior was observed during the induction reaction on NZ-20. The shorter diffusion path length combined with the larger external surface area of the catalyst promoted the diffusion of the aromatic molecules and further prevented the aggregation of too many retained species which are responsible for the deactivation at low temperature.

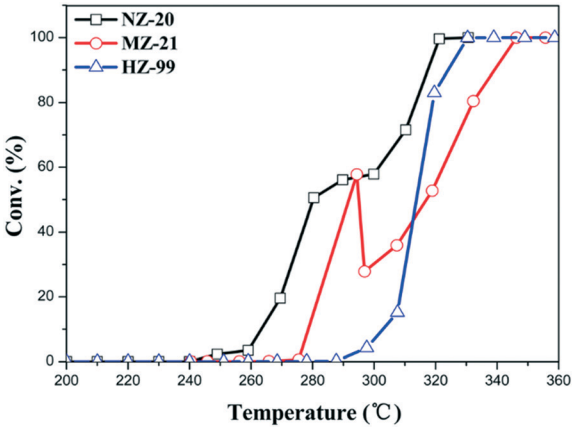


Fig. 5 Methanol conversion profiles as a function of temperature for HZ-99, MZ-21 and NZ-20 catalysts during the TP-MTH reaction.

## Conclusions

In summary, during the TP-MTH reaction, the evolution of catalyst activity with a linear increase of temperature was carefully monitored. Four different reaction stages could be clearly observed: the initial reaction stage, the auto-catalysis reaction stage, the deactivation stage and the activity recovery stage. An unusual deactivation behavior was observed following the auto-catalysis period. It was proved that the deactivation was not caused by the formation of usual "coke" species or other inactive residues but due to the accumulation of too many reactive centers. This phenomenon makes us reconsider the role of HCP compounds and propose the "overloading" effect: the promoting effect will not always increase with the increasing amount of active retained species due to the diffusivity limitation of the zeolite; on the contrary, too many active species will lead to catalyst deactivation at low temperature because of the serious occupation of the zeolite channels. Further study demonstrated that the "overloading effect" can be alleviated or eliminated by enhancing the catalyst diffusivity or decreasing the acid site density of the zeolite catalyst.

## Acknowledgements

The authors thank the financial support from the National Natural Science Foundation of China (No. 21576256 and No. 21273005).

## Notes and references

1 M. Stocker, *Microporous Mesoporous Mater.*, 1999, **29**, 3–48.
2 J. F. Haw, W. G. Song, D. M. Marcus and J. B. Nicholas, *Acc. Chem. Res.*, 2003, **36**, 317–326.
3 K. Y. Lee, H. K. Lee and S. K. Ihm, *Top. Catal.*, 2010, **53**, 247–253.
4 P. Tian, Y. X. Wei, M. Ye and Z. M. Liu, *ACS Catal.*, 2015, **5**, 1922–1938.
5 I. M. Dahl and S. Kolboe, *J. Catal.*, 1994, **149**, 458–464.
6 S. Svelle, F. Joensen, J. Nerlov, U. Olsbye, K. P. Lillerud, S. Kolboe and M. Bjorgen, *J. Am. Chem. Soc.*, 2006, **128**, 14770–14771.
7 M. Bjorgen, S. Svelle, F. Joensen, J. Nerlov, S. Kolboe, F. Bonino, L. Palumbo, S. Bordiga and U. Olsbye, *J. Catal.*, 2007, **249**, 195–207.
8 I. M. Dahl and S. Kolboe, *Catal. Lett.*, 1993, **20**, 329–336.
9 W. G. Song, J. F. Haw, J. B. Nicholas and C. S. Heneghan, *J. Am. Chem. Soc.*, 2000, **122**, 10726–10727.
10 K. Hemelsoet, J. Van der Mynsbrugge, K. De Wispelaere, M. Waroquier and V. Van Speybroeck, *ChemPhysChem*, 2013, **14**, 1526–1545.
11 S. Ilias and A. Bhan, *J. Catal.*, 2012, **290**, 186–192.
12 U. Olsbye, S. Svelle, M. Bjorgen, P. Beato, T. V. W. Janssens, F. Joensen, S. Bordiga and K. P. Lillerud, *Angew. Chem., Int. Ed.*, 2012, **51**, 5810–5831.
13 K. De Wispelaere, K. Hemelsoet, M. Waroquier and V. Van Speybroeck, *J. Catal.*, 2013, **305**, 76–80.
14 M. Westgard Erichsen, S. Svelle and U. Olsbye, *J. Catal.*, 2013, **298**, 94–101.
15 S. Ilias and A. Bhan, *J. Catal.*, 2014, **311**, 6–16.
16 T. Xu and J. F. Haw, *J. Am. Chem. Soc.*, 1994, **116**, 7753–7759.
17 T. Xu, D. H. Barich, P. W. Goguen, W. G. Song, Z. K. Wang, J. B. Nicholas and J. F. Haw, *J. Am. Chem. Soc.*, 1998, **120**, 4025–4026.
18 W. G. Song, H. Fu and J. F. Haw, *J. Phys. Chem. B*, 2001, **105**, 12839–12843.
19 W. G. Song, J. B. Nicholas and J. F. Haw, *J. Phys. Chem. B*, 2001, **105**, 4317–4323.
20 S. T. Xu, A. M. Zheng, Y. X. Wei, J. R. Chen, J. Z. Li, Y. Y. Chu, M. Z. Zhang, Q. Y. Wang, Y. Zhou, J. B. Wang, F. Deng and Z. M. Liu, *Angew. Chem., Int. Ed.*, 2013, **52**, 11564–11568.
21 W. O. Haag, R. M. Lago and P. G. Rodewald, *J. Mol. Catal.*, 1982, **17**, 161–169.
22 W. L. Dai, M. Scheibe, L. D. Li, N. J. Guan and M. Hunger, *J. Phys. Chem. C*, 2012, **116**, 2469–2476.
23 X. Y. Sun, S. Mueller, H. Shi, G. L. Haller, M. Sanchez-Sanchez, A. C. van Veen and J. A. Lercher, *J. Catal.*, 2014, **314**, 21–31.
24 L. Qi, Y. X. Wei, L. Xu and Z. M. Liu, *ACS Catal.*, 2015, **5**, 3973–3982.
25 J. F. Li, Z. H. Wei, Y. Y. Chen, B. Q. Jing, Y. He, M. Dong, H. J. Jiao, X. K. Li, Z. F. Qin, J. G. Wang and W. B. Fan, *J. Catal.*, 2014, **317**, 277–283.
26 F. F. Wei, Z. M. Cui, X. J. Meng, C. Y. Cao, F. S. Xiao and W. G. Song, *ACS Catal.*, 2014, **4**, 529–534.
27 W. L. Dai, C. M. Wang, M. Dyballa, G. J. Wu, N. J. Guan, L. D. Li, Z. K. Xie and M. Hunger, *ACS Catal.*, 2015, **5**, 317–326.
28 Y. X. Wei, D. Z. Zhang, F. X. Chang and Z. M. Liu, *Catal. Commun.*, 2007, **8**, 2248–2252.
29 Y. Liu, S. Muller, D. Berger, J. Jelic, K. Reuter, M. Tonigold, M. Sanchez-Sanchez and J. A. Lercher, *Angew. Chem., Int. Ed.*, 2016, **55**, 5723–5726.
30 H. Schulz, *Catal. Today*, 2010, **154**, 183–194.
31 H. Schulz, S. W. Zhao and H. Kusterer, *Chemistry of Microporous Crystals*, 1991, vol. 60, pp. 281–290.

32 S. Nawaz, S. Kolboe and M. Stocker, *Natural Gas Conversion Ii*, 1994, vol. 81, pp. 393–398.
33 F. Bleken, M. Bjorgen, L. Palumbo, S. Bordiga, S. Svelle, K. P. Lillerud and U. Olsbye, *Top. Catal.*, 2009, **52**, 218–228.
34 C. Y. Yuan, Y. X. Wei, J. Z. Li, S. T. Xu, J. R. Chen, Y. Zhou, Q. T. Wang, L. Xu and Z. M. Liu, *Cuihua Xuebao*, 2012, **33**, 367–374.
35 H. Schulz and M. Wei, *Microporous Mesoporous Mater.*, 1999, **29**, 205–218.
36 Y. X. Wei, J. Z. Li, C. Y. Yuan, S. T. Xu, Y. Zhou, J. R. Chen, Q. Y. Wang, Q. Zhang and Z. M. Liu, *Chem. Commun.*, 2012, **48**, 3082–3084.
37 E. Borodina, F. Meirer, I. Lezcano-Gonzalez, M. Mokhtar, A. M. Asiri, S. A. Al-Thabaiti, S. N. Basahel, J. Ruiz-Martinez and B. M. Weckhuysen, *ACS Catal.*, 2015, **5**, 992–1003.
38 T. Behrsing, H. Jaeger and J. V. Sanders, *Appl. Catal.*, 1989, **54**, 289–302.
39 L. Qi, J. Z. Li, Y. X. Wei, Y. L. He, L. Xu and Z. M. Liu, *RSC Adv.*, 2016, **6**, 52284–52291.
40 M. Abrishamkar and A. Izadi, *Microporous Mesoporous Mater.*, 2013, **180**, 56–60.
41 J. Huang, Y. Jiang, V. R. Marthala, Y. S. Ooi, J. Weitkarnp and M. Hunger, *Microporous Mesoporous Mater.*, 2007, **104**, 129–136.
42 Y. J. Jiang, J. Huang, V. R. R. Marthala, Y. S. Ooi, J. Weitkamp and M. Hunger, *Microporous Mesoporous Mater.*, 2007, **105**, 132–139.
43 W. L. Dai, M. Scheibe, N. J. Guan, L. D. Li and M. Hunger, *ChemCatChem*, 2011, **3**, 1130–1133.
44 W. L. Dai, X. Wang, G. J. Wu, N. J. Guan, M. Hunger and L. D. Li, *ACS Catal.*, 2011, **1**, 292–299.
45 M. Bjorgen, F. Bonino, S. Kolboe, K. P. Lillerud, A. Zecchina and S. Bordiga, *J. Am. Chem. Soc.*, 2003, **125**, 15863–15868.
46 W. L. Dai, G. J. Wu, L. D. Li, N. J. Guan and M. Hunger, *ACS Catal.*, 2013, **3**, 588–596.
47 W. Wang, Y. J. Jiang and M. Hunger, *Catal. Today*, 2006, **113**, 102–114.
48 C. Wang, Y. Y. Chu, A. M. Zheng, J. Xu, Q. Wang, P. Gao, G. D. Qi, Y. J. Gong and F. Deng, *Chem. – Eur. J.*, 2014, **20**, 12432–12443.
49 C. Wang, J. Xu, G. D. Qi, Y. J. Gong, W. Y. Wang, P. Gao, Q. Wang, N. D. Feng, X. L. Liu and F. Deng, *J. Catal.*, 2015, **332**, 127–137.
50 D. M. McCann, D. Lesthaeghe, P. W. Kletnieks, D. R. Guenther, M. J. Hayman, V. Van Speybroeck, M. Waroquier and J. F. Haw, *Angew. Chem., Int. Ed.*, 2008, **47**, 5179–5182.
51 H. Vankoningsveld, H. Vanbekkum and J. C. Jansen, *Acta Crystallogr., Sect. B: Struct. Sci.*, 1987, **43**, 127–132.
52 B. P. C. Hereijgers, F. Bleken, M. H. Nilsen, S. Svelle, K. P. Lillerud, M. Bjorgen, B. M. Weckhuysen and U. Olsbye, *J. Catal.*, 2009, **264**, 77–87.